Soft Matter

Cite this: *Soft Matter*, 2011, **7**, 7498

www.rsc.org/softmatter

PAPER

Detergency in a tube†

Keyvan Piroird,[ab] Christophe Clanet[ab] and David Quéré[ab]

Received 17th February 2011, Accepted 23rd May 2011
DOI: 10.1039/c1sm05282a

We study the motion of a drop of oil inside a capillary tube induced by a gradient of surfactant concentration. We first show that the wetting condition selects whether the drop moves towards or away from the surfactant. We then focus on the non-wetting case, for which the drop eventually escapes from the tube, and explore the different dynamics of propulsion. On a long time scale, we observe two regimes: either the drop reaches a constant velocity, or it moves intermittently, by successive jumps and stops. As a paradoxical consequence, viscous drops can be as mobile or even faster than inviscid ones.

Small amounts of surfactant can dramatically affect the hydrodynamics of a system. For example, as discussed by Levich, a bubble in water will rise more slowly if surfactants are present, due to the rigidification of the water/air interface.[1,2] In the same vein, several studies have shown that the pressure needed to displace a liquid slug inside a capillary tube is higher when surfactants are present, owing to the Marangoni stress they generate.[3–5] This stress also thickens the film deposited behind a bubble moving in a tube.[4,6] Surfactants can be exploited in enhanced oil recovery where the injection of soapy water helps to extract the residual oil trapped in the pores of a rock.[7,8] The use of surface-active molecules can also favor spontaneous motions of drops on solids,[9] or of small rafts at a liquid surface: in camphor boats, a traditional toy, camphor molecules placed on one side exert a pressure on the raft, which flees the surfactant source.[10,11]

We propose to use a surfactant-induced Marangoni force to propel a drop of oil inside a tube. Similar motions were observed by using thermal gradients, electrodes or by juxtaposing drops of different nature.[12–14] Here, the force is generated by a contrast in surfactant concentration between both sides of the drop. This experiment can be viewed as an elementary kind of detergency, where it is desired to displace oil inside pores until it leaves them.[15] We establish the conditions for achieving such a self-propelling system, and for sustaining it on large distances.

A first experiment consists of immersing a long horizontal tube (of inner radius $R = 1.5$ mm) in a bath of pure water. A drop of silicone oil of viscosity $\eta = 5$ mPa s is inserted in the tube with a syringe, which fixes its centimetre-size length L. Then, a controlled volume of surfactant solution is injected in water on one side of the drop. The surfactant in this study is sodium dodecyl sulfate (SDS), at a concentration C ranging between 0.05 mM and 80 mM, the critical micellar concentration C^* being 8 mM. Two different tubes were used, allowing us to invert the oil/water wettability: either a silicone tube wetted by oil, or a glass tube wetted by water. In the latter case, hydrophilicity was enhanced by polishing the tube with Cerox 1650 (Rhodia) and treating it for 10 min with a 1 M solution of sodium hydroxide. The resulting contact angle of oil is found to be between 170 and 180°. We show in Fig. 1 chronophotographs of the system after injecting the soap solution to the left of the oil. In the first picture, the surfactant solution is colored.

It is observed that oil moves, and in a direction that depends on the wetting condition. (a) In a silicone tube, the slug flees the source of surfactants. Its velocity is constant (approximately 4 mm s^{-1}), and the motion proceeds on distances much larger than L. The length L itself decreases with time, a consequence of the deposition of a film behind the slug.[3] The drop is asymmetric: its trailing edge meets the solid tangentially, while its leading edge makes a significant dynamic angle on the tube wall. (b) In a glass tube, the drop moves towards the surfactant. Contrasting with case (a), it remains symmetric and its velocity varies as a function of time: it first accelerates, reaches a maximum speed of approximately 30 mm s^{-1} (nearly 10 times quicker than the wetting drop), and slows down before stopping once it ran by about one unit in drop length L. (c) If the non-wetting oil reaches the end of the tube, it spontaneously escapes, since a drop has a smaller surface energy than a slug: the solid is clean of any oil at the end of the experiment.

The presence of surfactant on one side of the drop induces a Laplace pressure difference across the oil, whose sign is determined by the curvature of the menisci. Hence there is a pressure gradient $2\Delta\gamma/RL$ (in absolute value) between both menisci, where $\Delta\gamma = \gamma_o - \gamma$ is the difference in oil/water surface tension with and without surfactant. We measured $\gamma_o = 35 \pm 1$ mN m^{-1} (independent of the oil viscosity), and $\gamma = 5 \pm 1$ mN m^{-1} in the presence of SDS, above the critical micellar concentration. The force acting on the oil slug thus can be written:

[a]*Ladhyx, UMR 7646 du CNRS, École Polytechnique, 91128 Palaiseau Cedex, France*
[b]*Physique et Mécanique des Milieux Hétérogènes, UMR 7636 du CNRS, ESPCI, 75005 Paris, France*

† Electronic supplementary information (ESI) available. See DOI: 10.1039/c1sm05282a

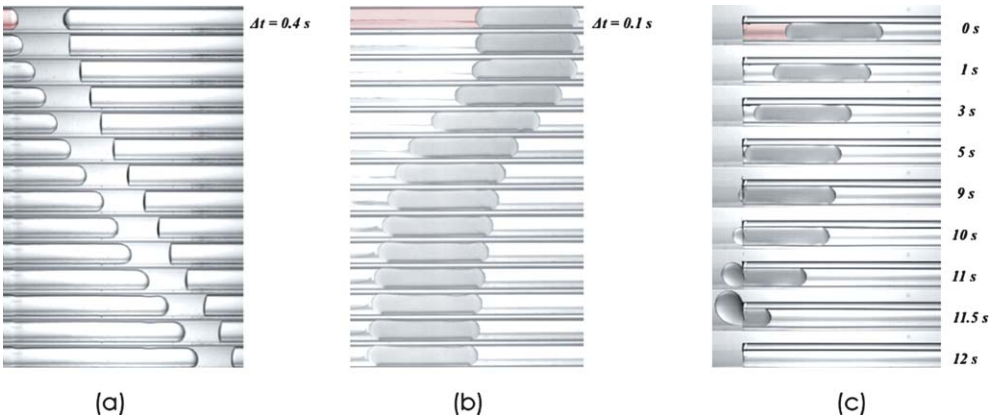

Fig. 1 Drop (length L) of silicone oil (viscosity $\eta = 5$ mPa s) in a tube (radius $R = 1.5$ mm) filled with water. SDS at a concentration of 10 C^* (where C^* is the critical micellar concentration) is injected on the left side, as symbolized by the color. (a) The tube is made of silicone, so that it is wetted by the oil slug ($L = 7.5$ mm), which moves away from the surfactant, at a constant velocity of 4 mm s^{-1}. Interval between successive images: 0.4 s. (b) The tube is made of clean glass, so that oil does not wet it. The slug (of length $L = 12$ mm) then moves towards the surfactant. It reaches a maximum velocity of 30 mm s^{-1} and it stops after a distance equal to L. Interval between successive images: 0.1 s. (c) The non-wetting oil spontaneously leaves the tube when it comes to its end (and then rises owing to gravity): the tube is clean of oil at the end of the experiment.

$$F = 2\pi R\Delta\gamma \quad (1)$$

Like in capillary rise, the sign of the capillary driving force F depends on the meniscus curvature: hence a motion in the right direction in case (a), and in the left direction in case (b). Eqn (1) can also be deduced from energetic arguments. As the slug moves along the tube axis x, it lowers its surface energy by an amount $2\pi Rx\Delta\gamma$, from which F can be derived.

The slug velocity depends on the friction law. As already emphasized, a wetting drop moves about 10 times slower than a non-wetting drop, which arises from the presence of contact lines.[16] Moving lines are known to induce a "special" enhanced friction – as commonly observed with drops sliding on planar solids.[17] There is no contact line in a non-wetting situation; instead, a water film lubricates the path for the slug, which yields larger velocities. The negligible deformation of the moving menisci (Fig. 1b) allows us to assume that eqn (1) (obtained from quasi-static arguments) can still hold in a dynamical regime. Contrasting with wetting oils (Fig. 1a), non-wetting drops are hardly deformed by the motion, due to a highly reduced friction in this case. This regime of non-wetting oils is the one on which we focus in this paper. It is interesting not only because slugs move faster, but also because it achieves a model situation of detergency, where oil gets evacuated from a confined structure without leaving a film behind: it somehow dewets the solid surface, and it even leaves the tube when it reaches its end (Fig. 1c). However, the presence of a water film around the oil slug induces a transfer of surfactant to the back of the slug, which may eventually stop the motion (end of the sequence in Fig. 1b). This can be seen as a serious limitation of the device, and we discuss below how this problem can be solved.

We measured the maximum velocity V of non-wetting oil drops (Fig. 1b) as a function of surfactant concentration C. Results are shown in Fig. 2a. At low concentration ($C \ll C^*$), V

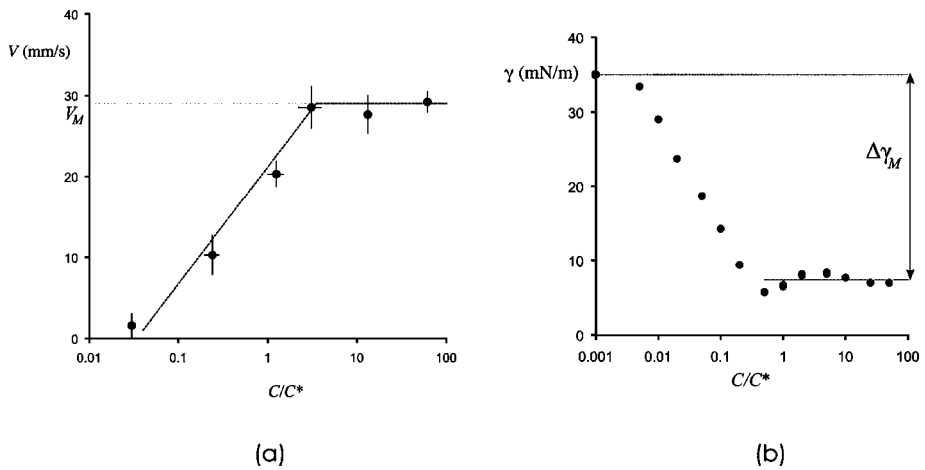

Fig. 2 (a) Maximum oil velocity V as a function of the surfactant concentration C normalized by the critical micellar concentration C^*. The non-wetting slug has a fixed length L =15 mm and a viscosity $\eta = 5$ mPa s. At high concentration, the velocity reaches a plateau value $V_M \approx 30$ mm s^{-1} (dashed line). (b) Oil/water surface tension as a function of concentration C, measured by the pendant drop method. In both plots, the concentration scale is logarithmic.

increases with the logarithm of C/C^*, which reflects the logarithmic dependence of the surface tension in this regime (Fig. 2b). At large concentration ($C \gg C^*$), the oil/water surface tension γ saturates; $\Delta\gamma$ reaches its maximum $\Delta\gamma_M$, and so does the velocity V. The plateau velocity V_M can be quite large (here approximately 30 mm s^{-1}, for a drop of length $L = 15$ mm and viscosity $\eta = 5$ mPa s), considering the confinement of the tube.

In order to understand the value V_M of the plateau velocity in Fig. 2a, we performed a series of measurements with oils of different viscosities (5 mPa s $< \eta <$ 5000 mPa s), and even with an air bubble ($\eta \approx 0.02$ mPa s, also non-wetting in a clean polished glass tube), for fixed slug length ($L = 15$ mm) and surfactant concentration ($C \approx 10C^*$). The results are displayed in Fig. 3, where we plotted the observed slug plateau velocity V_M (averaged on 2 to 3 similar experiments) as a function of its viscosity.

In this log-log plot, the slug velocity follows a scaling law $V_M \sim \eta^{-1}$ for $\eta > 50$ mPa s. This behavior suggests a balance between propulsion and viscous dissipation inside the oil, despite the presence of a lubricating film of water. The velocity profile in the oil slug can be tracked using tracers (Fig. 4). The flow is clearly not a plug flow as it could be without surfactants, when a viscous liquid flows on a film of smaller viscosity. Rather, the velocity profile is close to the parabolic Poiseuille profile drawn with a solid line. A detailed discussion (see appendix) confirms that velocity gradients can be concentrated in oil, owing to the existence of a surface tension gradient along the oil/water interface.

Assuming a Poiseuille flow inside the drop, the viscous force scales as $(\eta V/R^2)R^2L$, where R is the tube radius. Introducing the classical Poiseuille coefficient of 8π and balancing this force with (1) yields the slug velocity V:

$$V \approx \frac{\Delta\gamma R}{4\eta L} \qquad (2)$$

For $\Delta\gamma \approx \Delta\gamma_M \approx 30$ mN m^{-1}, $\eta \approx 1$ Pa s, $R \approx 1$ mm and $L \approx 1$ cm, we expect a plateau velocity V_M on the order of 1 mm s^{-1} and

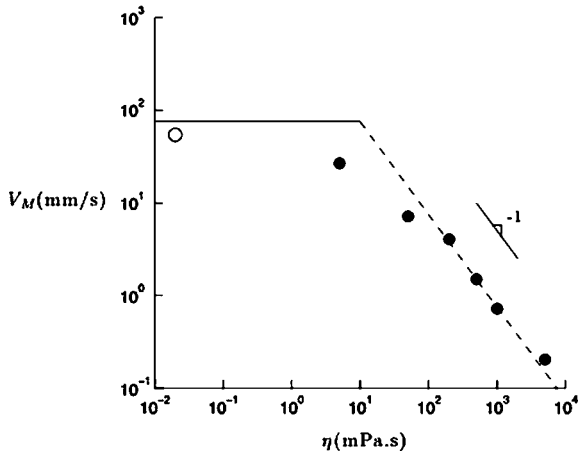

Fig. 3 Plateau drop velocity V_M as a function of oil viscosity η at high surfactant concentration ($C \approx 10C^*$). The empty symbol corresponds to measurements done with an air bubble, instead of oil slugs (full symbols). The drop (or bubble) has a fixed length $L = 15$ mm. The dashed line shows eqn (2) (see also eqn (A4) in the appendix), and the solid line eqn (3).

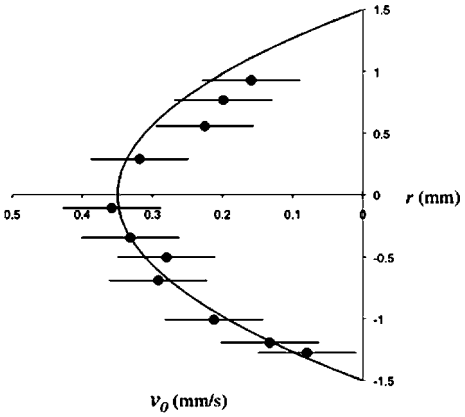

Fig. 4 Following tracers inside the moving slug allows us to extract the velocity profile inside the oil: v_o is the local velocity in oil, and r the radial coordinate. It is fairly well fitted by a parabolic Poiseuille profile, drawn with a solid line. In this experiment, the silicone oil has a viscosity $\eta =$ 5000 mPa s, the tube radius R is 1.5 mm, the SDS concentration responsible for the motion is 10 C^*.

decaying as $1/\eta$, as observed in Fig. 3, where eqn (2) is drawn with a dashed line.

Viscous dissipation takes place both in the slug and in water (of viscosity η_w). For a tube of total length L_T ($L_T \gg L$), the Stokes force in water $\eta_w V L_T$ exceeds the viscous force $\eta V L$ in the slug provided that $\eta < \eta_w L_T/L$. This condition is largely fulfilled if the slug is made of air, whose viscosity is 100 times smaller than that of water, while we have $L_T \approx 10L$. Balancing the corresponding Poiseuille force $8\pi\eta_w V L_T$ with the capillary force (1) yields a velocity:

$$V \approx \frac{\Delta\gamma R}{4\eta_w L_T} \qquad (3)$$

For our parameters ($\Delta\gamma \approx 30$ mN m^{-1}, $R \approx 1$ mm, $L \approx 1$ cm and $L_T \approx 10$ cm), we find $V \approx 7.5$ cm s^{-1}, drawn with a solid line in Fig. 3. We checked that the bubble velocity in this regime decreases with the tube length, confirming the role of the water flow in this limit of inviscid slugs. More sophisticated models might incorporate water dissipation at the entrance and exit of the tube, in particular for small tube lengths. The meniscus deformation might also be questioned: as it moves, the slug forms a liquid corner close to the wall. Characterizing this wedge by a dynamic contact angle θ, the associated viscous dissipation can be written $2\pi R\eta_w V/\theta$, where we have: $\theta \sim (\eta_w V/\gamma)^{1/3}$ (Tanner's law).[16] Hence the wedge friction scales as $2\pi R\gamma(\eta_w V/\gamma)^{2/3}$, which only induces a small correction to the force $F = 2\pi R\Delta\gamma$ (eqn (1)) for capillary numbers $\eta_w V/\gamma$ on the order of 10^{-3}, as in our experiments.

The slug velocity does not remain constant in the experiment, as illustrated in Fig. 1b. Owing to the presence of a wetting film of water, surfactant molecules are transported to the trailing edge of the drop, which eventually makes it stop. The movement thus seems to be limited (the slug is only translated by its own length), an obvious drawback for applications. However, this natural disadvantage can be overcome in two different ways. In Fig. 5, we show long-term sequences (over minutes), where we compare the behavior of oil drops of different viscosities (5 and 500 mPa s,

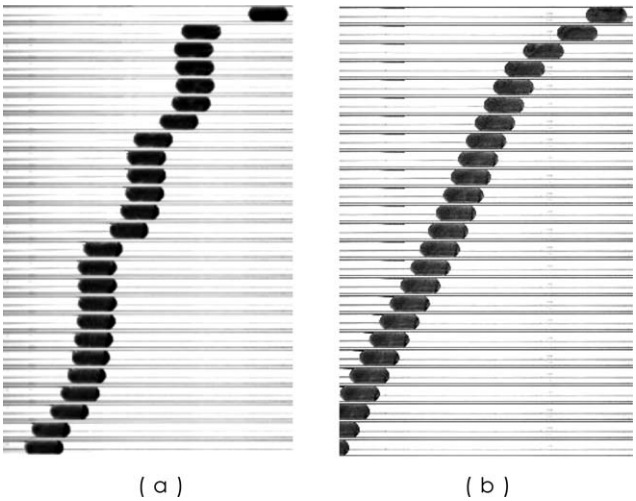

Fig. 5 Position of oil drops (length $L = 8$ mm, radius $R = 1.5$ mm) at long time scale. (a) $\eta = 5$ mPa s: the slug moves by successive jumps of order L, and it stops for a few tens of seconds between two jumps. (b) $\eta = 500$ mPa s: the slug first moves at 0.7 mm s^{-1}, and it selects after a distance of order L a constant velocity of 0.2 mm s^{-1}. Successive images are separated by 10 s in both figures. The SDS concentration on the left of the slug is $10C^*$.

respectively), placed in the same glass tube with the same surfactant asymmetry.

For the less viscous oil ($\eta = 5$ mPa s in Fig. 5a), the slug first quickly moves by a distance roughly equal to its length; then it stops for about one minute before jumping again, and so on, until it reaches the end of the tube, after 4 to 5 min. This "stick-and-slip" behavior contrasts with what is observed with the viscous oil ($\eta = 500$ mPa s in Fig. 5b). The drop first reaches the "maximum" velocity described previously (eqn (2)), corresponding to the three first images in the sequence of Fig. 5b. Then, it slows down and selects another velocity $V = 0.2$ mm s^{-1} and the motion remains stationary until the end of the tube (from which oil eventually escapes, like in the non-viscous case, Fig. 1c). The whole motion is found to be quicker than for a drop 100 times less viscous! Camphor-propelled boats were also observed to move continuously or intermittently, depending on the position of the camphor relative to the boat center.[10] Contrasting with our experiments, the "surfactant" in the latter case pushes the boat, and the motion is analyzed by balancing camphor sublimation with diffusion.

The behaviors in Fig. 5 might be explained as follows. In the first case (Fig. 5a), the quick motion favors the transport of surfactant to the trailing edge of the drop, through the wetting film along the tube. The surfactant concentration becomes comparable on both sides, and the motion stops. Then, the water film thins, and oil can weakly pin on the tube walls (contact angle close to 180°, yet slightly smaller). At the back, surfactants diffuse in pure water so that the surfactant concentration decreases as a function of time: a new pressure gradient builds up, which explains how motion can be reinitiated, once the force F exceeds the force necessary to depin the slug.

In the second case (Fig. 5b), the motion is initially much slower (due to the large oil viscosity, eqn (2)), and the amount of surfactant transported through the much thinner wetting film can be small enough to get simultaneously diluted by diffusion in fresh water, making possible a continuous motion. Then the velocity should be given by eqn (2), where $\Delta\gamma < \Delta\gamma_M$ is the surface tension difference between the slug ends in this stationary regime. We can compare the amounts of surfactant carried by the film and lost by diffusion in a control box of typical size R located at the trailing end of the slug, as shown in Fig. 6.

On the one hand, if the slug moves continuously at a velocity V (Fig. 5b), the water film of thickness h transports per unit time a flux $\phi_{in} \sim CRhV$. On the other hand, the diffusive flux ϕ_{out} of surfactant in a tube of characteristic radius R scales as CDR, where D is the diffusion coefficient of SDS in water, typically of order 10^{-10} m^2 s^{-1}. The Peclet number $Pe = \phi_{in}/\phi_{out} \sim hV/D$ compares the magnitude of these two fluxes. If this ratio is smaller than unity, diffusion is dominant and we expect a uniform motion. Conversely, a large Peclet number implies a convection-dominated transport, which yields an intermittent motion. In order to properly evaluate Pe, we need to determine the thickness of the dynamic film of water. For long slugs (of length $L \gg R$), the film thickness results from a balance between viscous friction (of water on the wall tube) and surface tension (which opposes the formation of the film), which leads to the so-called Bretherton law: $h \sim R(\eta_w V/\gamma)^{2/3}$, where η_w and γ stand for the water viscosity and oil/water surface tension.[3,18] The scaling of this law remains the same if the viscosity η of the surrounding medium (oil, here) is much larger than η_w (like in Fig. 5b), the only difference being a modification of the numerical coefficient.[19] The same remark applies if surfactant molecules are present along the oil/water interface.[4]

The slug velocity highly depends on the oil viscosity (eqn (2)), so that we expect a significant difference in the film thickness between the two experiments in Fig. 5. More precisely, Bretherton law predicts a film of 50 μm for the low oil viscosity ($\eta = 5$ mPa s), instead of 1 μm for the high viscosity ($\eta = 500$ mPa s). As a consequence, the number $Pe = hV/D$ is dramatically different in both experiments: while it is on the order of 10^4 for the oil of low viscosity, it becomes of order 1 for the more viscous one. This is the limit below which we expect the possibility of diluting the surfactant behind the drop as the movement proceeds, leading to a continuous motion. For viscous oils ($\eta > 50$ mPa s), we can combine the definition of the Peclet number with Bretherton's law and eqn (2), which provides a general expression: we find $Pe \sim R^{8/3}/L^{5/3}a$, where the length a only depends on the nature of the fluids and surfactant ($a = D\gamma^{2/3}\eta^{5/3}/\eta_w{}^{2/3}\Delta\gamma^{5/3}$). In the experiment of Fig. 5, continuous motion is triggered by increasing

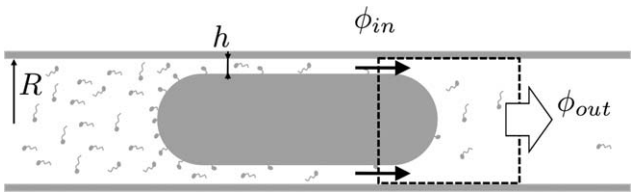

Fig. 6 Surfactant balance in a control box of typical size R located at the trailing end of the slug, shown in dotted line. ϕ_{in} is the incoming flux of surfactant through the lubricating film of water and ϕ_{out} is the outgoing diffusive flux.

a through the oil viscosity, on which it depends strongly, as $\eta^{5/3}$. The same trend is expected by reducing the tube radius ($Pe \sim R^{8/3}$), or by increasing the slug length ($Pe \sim L^{-5/3}$), making continuous motions (and detergency) possible in various situations.

We checked these predictions with an oil of intermediate viscosity ($\eta = 100$ mPa s). For the geometric features of Fig. 5 (slug length $L = 8$ mm, tube radius $R = 1.5$ mm), the corresponding Peclet number is 15 ($\gg 1$) and we indeed observe an intermittent motion, as seen in Fig. 7 where we plot the slug position as a function of time (solid line). After a jump of length L, the drop stops for a few minutes before new jumps-and-stops. We did the same experiment in a tube of radius $R = 0.5$ mm, which lowers the Peclet number by a factor 20. As expected, the motion then becomes continuous (dashed line in Fig. 7). As a paradoxical consequence, the time needed for travelling on a distance of 50 mm is lowered by a factor 4, despite a more confined tube! In the same spirit, if the slug in the tube of radius $R = 1.5$ mm is 2.5 times longer, the Peclet number is significantly decreased (by a factor 5), and the motion also becomes (roughly) continuous (dotted line): again, the velocity decreases for $x > L = 2$ cm, but there is no stop, and the motion proceeds along the whole tube.

In summary, we showed that an inhomogeneous surfactant concentration can propel a drop inside a tube, in a direction determined by the tube wettability. We focused on the non-wetting case where the drop velocity increases with surfactant concentration and reaches a constant value at high surfactant concentration. This value results from a balance between capillary propulsion and viscous dissipation, either in oil of viscosity larger than ~50 mPa s or in water at small slug viscosity. On long time scales, the motion is either uniform or intermittent. We proposed an explanation that takes into account surfactant flux through the lubricating film, and discussed more specifically why and how continuous propulsion can be generated.

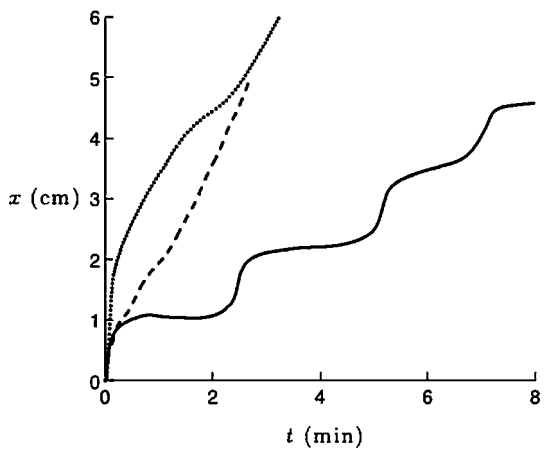

Fig. 7 Position of a slug of viscosity $\eta = 100$ mPa s as a function of time. The motion is intermittent for wide tubes and short slugs ($R = 1.5$ mm and $L = 8$ mm, solid line), but it can be made continuous (and thus much quicker) either by increasing the slug length ($R = 1.5$ mm and $L = 20$ mm, dotted line), or by decreasing the tube radius ($R = 0.5$ mm and $L = 8$ mm, dashed line). The SDS concentration ahead is $10C^*$.

Appendix – on the viscous slug velocity

We discuss here the regime of high slug viscosity η, corresponding to Fig. 4 and 5b, and to eqn (2). As seen in the text, this regime corresponds to $\eta > \eta_w L_T/L$ (where η_w is the water viscosity, L the slug length, and L_T the tube length), that is, to oil viscosities larger than about 10 times the water viscosity in our experiments. We choose the reference frame in which the slug does not move and calculate the flow profile, assuming that inertia is negligible. In a tube of radius R where x and r are the longitudinal and radial coordinates, oil and water are located between $r = 0$ and $R - h$, and $R - h$ and R, respectively. In this system, the pressure gradient is only present in the oil phase where we expect a Poiseuille flow far from the ends of the slug. There is no pressure gradient in the water phase (the tube is open at both ends), which yields a Couette flow in the water film. Hence we get the velocity profile in each phase:

$$\begin{aligned} v_o(r) &= \frac{\Delta\gamma}{2\eta}\frac{r^2}{(R-h)L} + A \qquad \text{for } 0 < r < R-h \\ v_w(r) &= B\ln r + C \qquad \text{for } R-h < r < R \end{aligned} \tag{A1}$$

where A, B and C are integration constants. In the chosen reference frame, conservation of mass for the slug can be written: $\int_0^{R-h} v_o(r) 2\pi r \, dr = 0$, from which we get $A = -\Delta\gamma(R-h)/4\eta L$. As for the stress continuity equation at the interface, we must take into account the additional stress due to the gradient of surfactant along the slug, which is equal to $\Delta\gamma/L$. It comes:

$$\eta_w \left.\frac{dv_w}{dr}\right|_{R-h} = \eta \left.\frac{dv_o}{dr}\right|_{R-h} - \frac{\Delta\gamma}{L} \tag{A2}$$

Hence we find $B = 0$: the velocity profile is constant in the water phase. The gradient of surface tension along the drop induces a pressure gradient in oil proportional to $\Delta\gamma/L$ and it generates a bulk flow towards decreasing values of x; but this gradient also creates a Marangoni stress at the water/oil interface proportional to $\Delta\gamma/L$ and responsible for a surface flow in the opposite direction. Those two effects exactly compensate each other. Finally, the velocity continuity at the interface yields: $C = \Delta\gamma(R-h)/4\eta L$.

The velocity field sketched in Fig. 8 can be written explicitly:

$$\begin{aligned} v_o(r) &= \frac{\Delta\gamma}{2\eta L}\left(\frac{r^2}{R-h} - \frac{R-h}{2}\right) \qquad \text{for } 0 < r < R-h \\ v_w(r) &= \frac{\Delta\gamma(R-h)}{4\eta L} \qquad \text{for } R-h < r < R \end{aligned} \tag{A3}$$

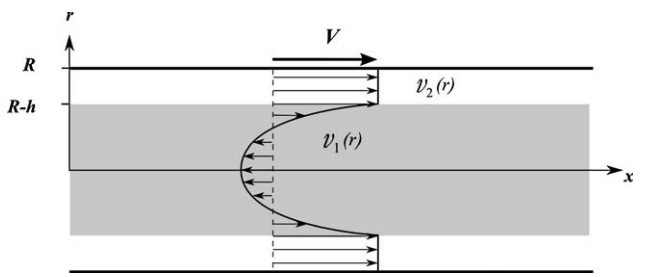

Fig. 8 Velocity profile in oil and water in the frame of reference of the slug, as described by eqn (A3). The mean velocity of the oil phase is equal to zero and the velocity profile in water is constant because viscous and Marangoni stresses balance at the oil/water interface.

The flow is very different from a plug flow, which could be observed in the absence of surfactants. In our case, the velocity gradients are located in the oil phase (Fig. 4). In the reference frame of the tube, the velocity profile is constant and equal to 0 in the water film. Hence we do not expect any motion of the oil slug if an end of the tube is closed, which we checked experimentally.

The slug velocity is $V = v_w(R) = \Delta\gamma(R - h)/4\eta L$. The film thickness itself is a function of V, as shown by Bretherton: $h \sim R(\eta_w V/\gamma)^{2/3}$ where γ is the oil/water surface tension in presence of surfactant ($\sim$5 mN m^{-1}).[3,18] As mentioned in text, this scaling still holds for $\eta \gg \eta_w$, and if surfactant molecules are present along the oil/water interface.[4,19] Since the capillary number corresponding to our experiments is smaller than 10^{-2}, the water film is always much thinner than the tube radius ($h \ll R$), so that the velocity V simply is:

$$V = \frac{\Delta\gamma R}{4\eta L} \quad \text{(A4)}$$

This law (eqn (2)) is drawn with a dotted line in Fig. 3 where it provides a good agreement with the data for $\eta > 50$ mPa s, without any adjustable parameter. We can finally notice that the flow of water generates a pressure gradient in water, which seems in contradiction with the plug profile we found. This pressure gradient scales as $\eta_w V/R^2$, and thus implies a pressure difference in water of $\eta_w V L_T/R^2$. This correction is negligible compared to the other terms in the equations, provided that $\eta > \eta_w L_T/L$, the condition assumed in this section.

References

1 B. Levich, *Physicochemical hydrodynamics*, 1962, Prentice Hall, Englewood Cliffs.
2 C. Ybert and J. M. di Meglio, *Eur. Phys. J. B*, 1998, **4**, 313–319.
3 F. P. Bretherton, *J. Fluid Mech.*, 1961, **10**, 166–188.
4 J. Ratulowski and H. C. Chang, *J. Fluid Mech.*, 1990, **210**, 303–328.
5 B. Dollet and I. Cantat, *J. Fluid Mech.*, 2010, **652**, 529–539.
6 B. Scheid *et al.*, *Europhys. Lett.*, 2010, **90**, 24002.
7 T. Austad, B. Matre, J. Milter, A. Sævareid and L. Øyno, *Colloids Surf., A*, 1998, **137**, 117–129.
8 N. R. Morrow and G. Mason, *Curr. Opin. Colloid Interface Sci.*, 2001, **6**, 321–337.
9 Y. Sumino, N. Magome, T. Hamada and K. Yoshikawa, *Phys. Rev. Lett.*, 2005, **94**, 068301.
10 S. Nakata, Y. Doi and K. Kitahata, *J. Phys. Chem. B*, 2005, **109**, 1798–1802.
11 N. J. Suematsu, Y. Ikura, M. Nagayama, H. Kitahata, N. Kawagishi, M. Murakami and S. Nakata, *J. Phys. Chem. C*, 2010, **114**, 9876–9882.
12 E. Lajeunesse and G. M. Homsy, *Phys. Fluids*, 2003, **15**, 308–314.
13 M. G. Pollack, R. B. Fair and A. D. Shenderov, *Appl. Phys. Lett.*, 2000, **77**, 1725–1726.
14 J. Bico and D. Quéré, *J. Fluid Mech.*, 2002, **467**, 101–127.
15 A. W. Sonesson, T. H. Callisen, U. M. Elofsson and H. Brismar, *J. Surfactants Deterg.*, 2007, **10**, 211–218.
16 J. Bico and D. Quéré, *J. Colloid Interface Sci.*, 2001, **243**, 262–264.
17 N. Le Grand, A. Daerr and L. Limat, *J. Fluid Mech.*, 2005, **541**, 293–315.
18 P. Aussillous and D. Quéré, *Phys. Fluids*, 2000, **12**, 2367–2371.
19 L. W. Schwartz, H. M. Princen and A. D. Kiss, *J. Fluid Mech.*, 1986, **172**, 259–275.